

RESEARCH PAPER

RecA maintains the integrity of chloroplast DNA molecules in *Arabidopsis*

Beth A. Rowan[†], Delene J. Oldenburg and Arnold J. Bendich*

Department of Biology, University of Washington, Seattle, WA 98195 USA

[†] Present address: Department of Molecular Biology, Max Planck Institute for Developmental Biology, D-72076 Tübingen, Germany.

* To whom correspondence should be addressed. E-mail: bendich@u.washington.edu

Received 28 January 2010; Revised 15 March 2010; Accepted 16 March 2010

Abstract

Although our understanding of mechanisms of DNA repair in bacteria and eukaryotic nuclei continues to improve, almost nothing is known about the DNA repair process in plant organelles, especially chloroplasts. Since the RecA protein functions in DNA repair for bacteria, an analogous function may exist for chloroplasts. The effects on chloroplast DNA (cpDNA) structure of two nuclear-encoded, chloroplast-targeted homologues of RecA in *Arabidopsis* were examined. A homozygous T-DNA insertion mutation in one of these genes (*cpRecA*) resulted in altered structural forms of cpDNA molecules and a reduced amount of cpDNA, while a similar mutation in the other gene (*DRT100*) had no effect. Double mutants exhibited a similar phenotype to *cpRecA* single mutants. The *cpRecA* mutants also exhibited an increased amount of single-stranded cpDNA, consistent with impaired RecA function. After four generations, the *cpRecA* mutant plants showed signs of reduced chloroplast function: variegation and necrosis. Double-stranded breaks in cpDNA of wild-type plants caused by ciprofloxacin (an inhibitor of *Escherichia coli* gyrase, a type II topoisomerase) led to an alteration of cpDNA structure that was similar to that seen in *cpRecA* mutants. It is concluded that the process by which damaged DNA is repaired in bacteria has been retained in their endosymbiotic descendent, the chloroplast.

Key words: DNA structure, fluorescence microscopy, homologous recombination, leaf variegation, pulsed-field gel electrophoresis.

Introduction

All organisms experience DNA damage, which must be repaired in order to avoid deleterious phenotypic consequences (Thompson and Schild, 2001; Tuteja *et al.*, 2009). Many processes can be used to maintain the integrity of the genome: photoreactivation, base excision repair, nucleotide excision repair, mismatch repair, homologous recombination, and cross-link repair (Sancar and Sancar, 1988; Niedernhofer, 2008). Mechanistic details are becoming increasingly clear in bacteria, eukaryotic nuclei, and the mitochondria of yeast and mammals (Bohr and Anson, 1999; Nowosielska, 2007; Aguilera and Gomez-Gonzalez, 2008). By comparison, however, DNA repair processes in the mitochondria and chloroplasts of plants remain poorly

understood (Kimura and Sakaguchi, 2006; Vlcek *et al.*, 2008).

Homologous recombination is important for the repair of double-strand DNA breaks (DSB), DNA gaps, and interstrand cross-links, and occurs by invasion of a homologous DNA strand followed by strand exchange (Li and Heyer, 2008). The *Escherichia coli* RecA/RecBCD pathway of strand invasion and exchange is perhaps the best characterized system for DNA repair by homologous recombination (Cox, 2007; Michel *et al.*, 2007). The RecA protein is highly conserved among diverse bacterial species, and the RecBCD complex has different functional analogues in different bacterial lineages (Rocha *et al.*, 2005).

Eukaryotic homologues of RecA (RAD51) and organelle-targeted prokaryotic RecA homologues are encoded by the nuclear genomes of many organisms, including plants (Lin et al., 2006). Repair and recombination of chloroplast DNA (cpDNA) in *Chlamydomonas reinhardtii* is suppressed when a dominant-negative version of *E. coli* RecA is targeted to chloroplasts (Cerutti et al., 1995). The prevalence of chloroplast-targeted *RecA* mRNA increases in response to DNA damage in *C. reinhardtii* (Nakazato et al., 2003), *Physcomitrella patens* (Inouye et al., 2008), pea (Cerutti et al., 1993), and *Arabidopsis* (Cao et al., 1997). Mitochondrial-targeted RecA has been shown to be important for mitochondrial DNA (mtDNA) repair in *P. patens* (Odahara et al., 2007) and for mtDNA recombination and repair in *Arabidopsis* (Khazi et al., 2003; Shedge et al., 2007).

The nuclear genome of *Arabidopsis* encodes five putative homologues of RecA that are predicted to be localized in mitochondria and chloroplasts (Table 1). Locus AT1G79050 encodes a protein (RECA1; cpRecA) that has been shown experimentally to be located in chloroplasts (Cao et al., 1997; Shedge et al., 2007) and has a 61% identity with cyanobacterial RecA (Cerutti et al., 1992). Locus AT3G12610 encodes a protein (DRT100) that has only weak homology to *E. coli* RecA and has a putative chloroplast-targeting signal peptide (Pang et al., 1992). *DRT100* cDNA can, however, partially restore the growth phenotypes of *recA* mutants of *E. coli* (Pang et al., 1992, 1993). Locus AT2G19490 encodes a protein (RECA2) that localizes to both mitochondria and chloroplasts, and locus AT3G10140 (RECA3) encodes a protein that localizes to mitochondria only (Shedge et al., 2007). Locus AT3G32920 has been annotated as encoding a mitochondrial-targeted RecA protein, but the gene is probably a pseudogene (Shedge et al., 2007).

Previous reports describing the consequences of mutation in a chloroplast-targeted *RecA* homologue for any plant could not be found [other than lethality previously reported for *RECA1/cpRecA* (Shedge et al., 2007)]. In this study, the function of two of the three chloroplast-targeted RecA proteins in *Arabidopsis* is addressed using T-DNA insertion mutants and it is shown that the *cpRecA* gene encodes a protein that functions similarly to bacterial RecA. Pulsed-field gel electrophoresis (PFGE) and fluorescence microscopy of individual ethidium bromide-stained cpDNA molecules were used to analyse cpDNA structure. In wild-type (wt) *Arabidopsis*, as in other plants, in-gel-prepared cpDNA consists of multigenomic, complex forms that do not

migrate into the gel, discrete bands of monomeric and oligomeric linear molecules, and a smear of linear molecules. Circular forms are rarely found. Reduction of *cpRecA* mRNA leads to a decrease in the prominence of the bands, an increase in the smear, and leaf abnormalities that probably result from a lack of DNA damage repair in chloroplasts.

Materials and methods

Plant growth conditions

Seeds of *Arabidopsis thaliana* (Columbia or SALK T-DNA insertion lines obtained from the Arabidopsis Biological Resource Center, <http://www.biosci.ohio-state.edu/~plantbio/Facilities/abrc/abrchome.htm>) were sown on soil (for the experiments shown in Figs 1–4) or on sterile agar plates containing MS salts (Murashige and Skoog, 1962), 1% sucrose, and 0, 0.5, 1, or 2 μM ciprofloxacin (for the experiments shown in Figs 5 and 6). Seeds were held at 4 °C for 3 d to promote uniform germination before transferring them to a greenhouse (soil) or growth room at 20 °C with constant light at 30 $\mu\text{Einsteins m}^{-2} \text{s}^{-1}$.

Obtaining homozygous T-DNA insertion mutants

Wt plants and plants homozygous for a T-DNA insertion near the 3' end (*drt100-1*) or in the middle (*drt100-2*) of the single exon in the *DRT100* gene were selected from SALK lines 021479 and 102492, respectively, using PCR-based genotyping. Primers to distinguish wt alleles from those containing the T-DNA insertion were designed using the T-DNA express tool at <http://signal.salk.edu/cgi-bin/tdnaexpress> (see Table 2). The wt plants and plants homozygous for a T-DNA insertion in the third to last exon of the *cpRecA* gene (*cprecA*) were selected similarly from SALK line 072979. Seeds from single individual homozygous plants (wt or *cprecA*; generation 1) were collected and raised to maturity (generation 2). Seeds from two individuals were then collected (generation 3) and used to produce the plants used for chloroplast isolation and PFGE experiments. Two individuals were selected at each generation starting at generation 3 to give rise to generations 4–7.

Measurement of mRNA levels for DRT100 and cpRecA using reverse transcriptase real-time quantitative PCR

RNA from shoots of 13-day-old seedlings was prepared using a Sigma Spectrum™ Plant Total RNA Kit, treated with DNase (DNA-free™ Kit, Applied Biosystems, http://www3.appliedbiosystems.com/AB_Home/index.htm) and reverse transcribed using the BioRad iScript™ cDNA synthesis kit (www.biorad.com). Amplification of 2 μl of cDNA was carried out using the BioRad iQ™ SYBR Green Supermix (www.biorad.com) with the primer sets described in Table 2. Following an initial denaturation at 94 °C for 3 min 15 s, 45 cycles of 20 s denaturation at 94 °C, 20 s annealing at 57 °C, and 30 s extension at 72 °C were

Table 1. Organelle-targeted homologues of bacterial RecA encoded by the *Arabidopsis* nuclear genome

Locus	Name	Compartment of gene product	Reference
AT1G79050	<i>RECA1</i> ; <i>cpRecA</i>	Chloroplast	Cerutti et al. (1992); Cao et al. (1997); Shedge et al. (2007)
AT3G12610	<i>DRT100</i>	Chloroplast	Pang et al. (1992, 1993)
AT2G19490	<i>RECA2</i>	Chloroplast; mitochondria	Shedge et al. (2007)
AT3G10140	<i>RECA3</i>	Mitochondria	Khazi et al. (2003); Shedge et al. (2007)
AT3G32920	None	Mitochondria ^a	Shedge et al. (2007)

^a Mitochondrial targeting based on NCBI GenBank annotation.

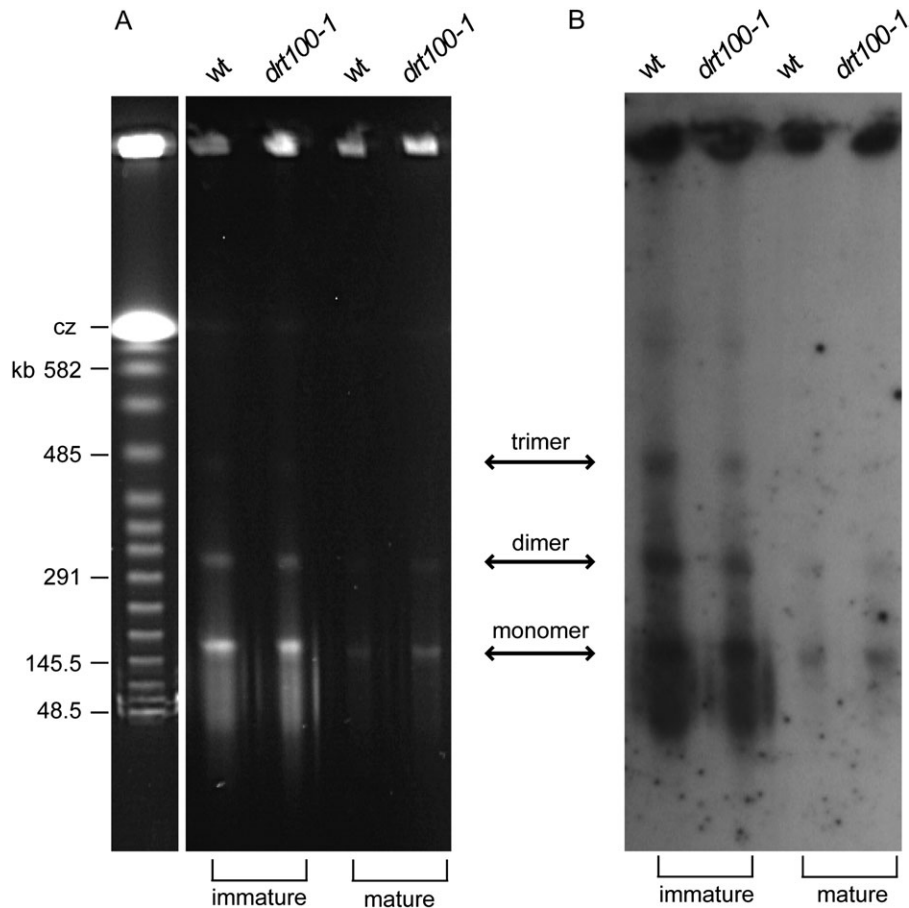


Fig. 1. The effect of a T-DNA insertion in *DRT100* on cpDNA amount and structure. (A) PFGE of cpDNA obtained from an equal volume of pelleted chloroplasts from wt and *dt100-1* mutant plants after staining with ethidium bromide. (B) Blot hybridization of the gel in (A) with an 854 bp cpDNA-specific probe that contains a portion of the *petA* gene. Similar results were obtained with a different T-DNA insertion allele (*dt100-2*; data not shown). Immature, entire shoots of plants grown for 16 d post germination; mature, third rosette leaves of plants grown for 30 d post-germination. The ratio of the hybridization signals for each of the lanes is 2.5:2.2:1:1.2 for wt immature:*dt100-1* immature:wt mature:*dt100-1* mature, respectively. Linear DNA sizes (in kb) are indicated. cz, compression zone.

performed, and amplification of the reactions was monitored using the Chromo 4 real-time detection system (Bio-Rad Laboratories, www.biorad.com). A melting curve from 65 °C to 95 °C was used to confirm the presence of single products. Data were analysed using the Opticon Monitor 3 software (Bio-Rad Laboratories, www.biorad.com) and the amount of each transcript was determined relative to the actin gene *ACT2* using the $2^{-\Delta CT}$ method (Livak and Schmittgen, 2001). The highest amount was assigned a value of 1 and all other values are expressed relative to 1.

Chloroplast isolation and preparation for PFGE and fluorescence microscopy

Tissue collected from plants grown in a greenhouse was washed for 3–5 min in 0.5% sarkosyl and rinsed exhaustively four times in tap water and four times in distilled water before isolating chloroplasts using the high-salt method that avoids using DNase (Shaver *et al.*, 2006; Rowan *et al.*, 2007). For PFGE and analysis of cpDNA molecules from individual chloroplasts, the isolated chloroplasts were embedded in agarose and lysed overnight at 48 °C in 1 M NaCl, 5 mM EDTA, 1% sarkosyl, and 200 $\mu\text{g ml}^{-1}$ proteinase K. Agarose plugs were washed extensively in many plug volumes of 10 mM TRIS, 1 mM EDTA (TE) before PFGE with 1.5% (w/v) agarose at 5 V cm^{-1} , in 45 mM TRIS, 45 mM boric acid, 1 mM EDTA, and a pulse time of 50 s. Prior to mung bean nuclease treatment, washed cpDNA–agarose plugs were treated

with 2 mM phenylmethylsulphonyl fluoride (PMSF) for 3 h, then treated with an additional 2 mM PMSF for 1 h. PMSF-treated cpDNA–agarose plugs were washed extensively in many plug volumes of TE before soaking in 30 mM sodium acetate, pH 7.5, 50 mM NaCl, 1 mM ZnCl_2 , 5% glycerol for 1 h on ice and treating with or without 2.5 U of mung bean nuclease for 15 min or 30 min at 37 °C in a total volume (liquid plus gel) of 120 μl . Digestion was stopped by adding 0.1% sarkosyl, 10 mM EDTA, pH 9. For analysis of cpDNA from individual chloroplasts, agarose-embedded cpDNA was prepared at a concentration 100- to 500-fold less than was used for PFGE, stained with 0.1 $\mu\text{g ml}^{-1}$ ethidium bromide, and visualized as described (Oldenburg and Bendich, 2004b). For estimation of genome equivalents per plastid, isolated chloroplasts were stained with 4',6-diamidino-2-phenylindole (DAPI) and the relative fluorescence intensity (Rfl) was measured as described (Rowan *et al.*, 2004, 2007). Rfl was determined similarly for glutaraldehyde-fixed, DAPI-stained vaccinia virus particles. The number of chloroplast genome equivalents per plastid was calculated using the equation: chloroplast genome equivalents = $1.33V$ (where V = the DAPI–DNA Rfl of the plastid divided by the mean Rfl of vaccinia virus particles). The value 1.33 is a constant that accounts for the differences between the size and base composition between the *Arabidopsis* chloroplast genome and the vaccinia virus genome, and was determined as $(\%AT \text{ content of vaccinia virus genome} / \%AT \text{ content of } Arabidopsis \text{ chloroplast genome}) \times (\text{number of bp of vaccinia virus}$

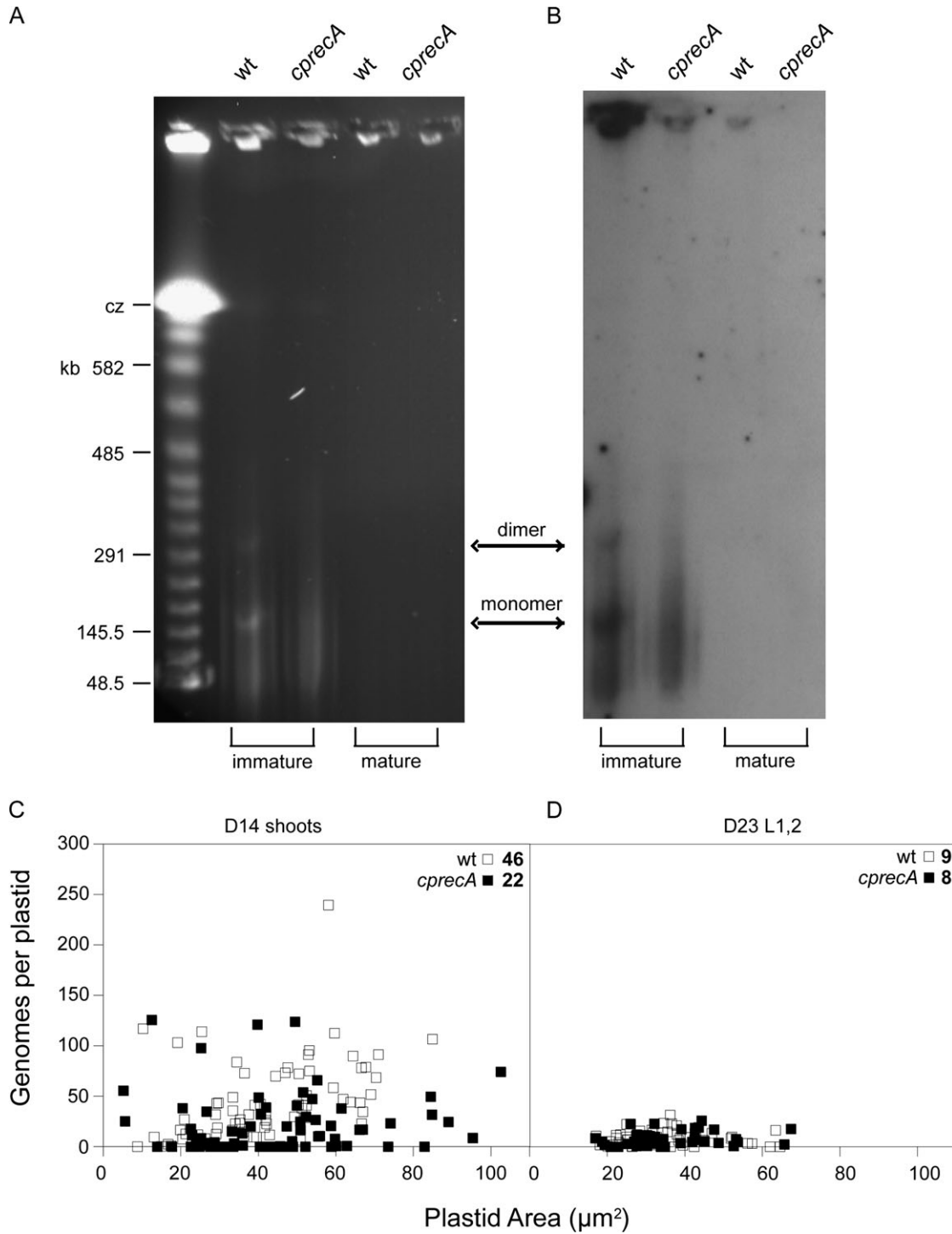


Fig. 2. The effect of a T-DNA insertion in *cpRecA* on cpDNA amount and structure. (A) PFGE of cpDNA obtained from an equal volume of pelleted chloroplasts from wt and *cprecA* mutant plants after staining with ethidium bromide. (B) Blot hybridization of the gel in (A) with a *petA* probe. Immature, entire shoots of plants grown for 14 d post-germination; mature, first and second rosette leaves from plants grown for 23 d post-germination. The ratio of the hybridization signals for each of the lanes is 6:3.8:1:1.3 for wt immature:*cprecA* immature:wt mature:*cprecA* mature, respectively. Linear DNA sizes (in kb) are indicated. cz, compression zone. (C and D) Size and DNA content of plastids isolated from wt and *cprecA* mutant plants. Genome equivalents per plastid were determined by DAPI staining, using vaccinia virus particles as a standard [results using this method are similar to those using real-time qPCR (Rowan *et al.*, 2009)]. D14 shoots, entire shoots of plants grown for 14 d post-germination. D23 L1,2, first and second rosette leaves from plants grown for 23 d post-germination. Numbers in the upper right corners of (C) and (D) represent the mean of genome equivalents per plastid. The mean μm^2 per plastid (and number of plastids analysed) at D14 are 42 (69) for wt and 45 (68) for *cprecA*. The corresponding values at D23 are 35 (51) for wt and 36 (44) for *cprecA*. The relative cpDNA amounts among samples are similar when assessed by quantification of the blot hybridization signal (B) and genome copy number (C and D).

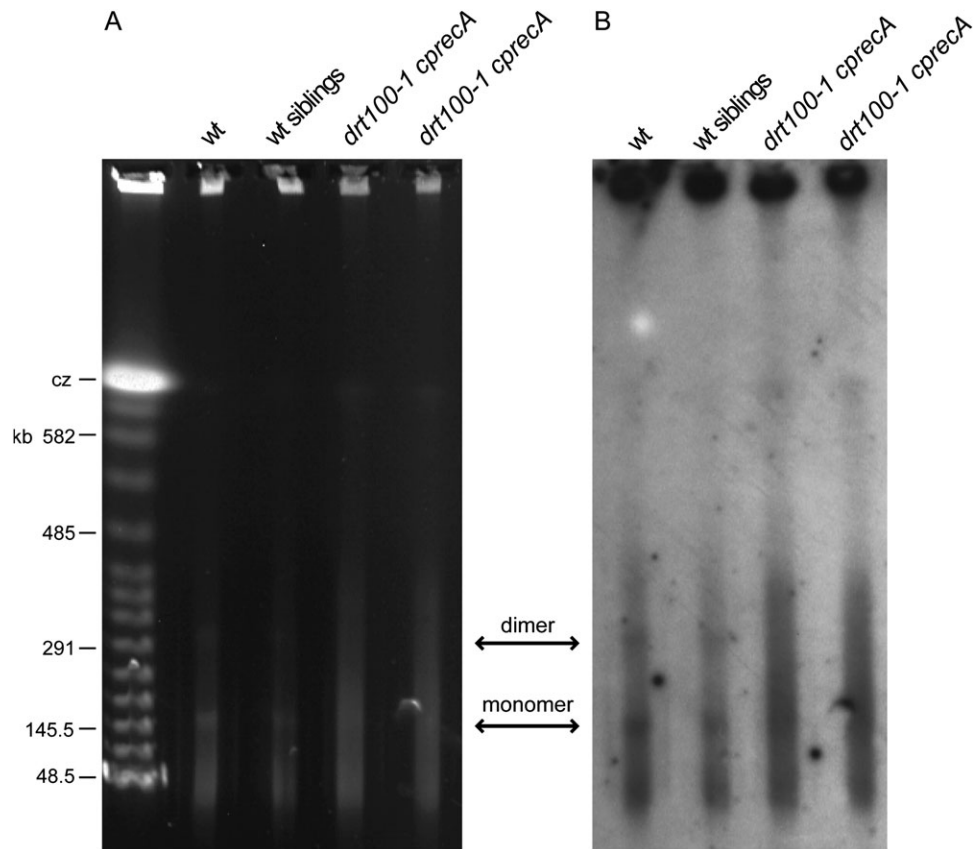


Fig. 3. Structure of cpDNA in *drt100-1 cprecA* double mutants. (A) PFGE of cpDNA obtained from an equal volume of pelleted chloroplasts after staining with ethidium bromide and (B) blot hybridization of the gel in (A) with a *petA* probe. The cpDNA from wt, wt siblings (F_3 wt siblings obtained from the F_2 segregating population), and *cprecA drt100-1* double mutants (two independent F_3 lines obtained from the F_2 segregating population) is indicated. As with *cprecA* single mutants (Fig. 2), the double mutants show no prominent bands of genomic monomers and dimers, and more of the DNA migrates as a smear compared with their wt siblings and unrelated wt (Col) plants. DNA was obtained from chloroplasts isolated from 13-day-old seedlings. Linear DNA sizes (in kb) are indicated. cz, compression zone.

genome/number of bp of *Arabidopsis* chloroplast genome), where %AT for vaccinia virus (Copenhagen strain) is 66.6, %AT for *Arabidopsis* cpDNA is 64%, number of bp for vaccinia virus DNA is 197361 and number of bp for *Arabidopsis* cpDNA is 154361. Brightfield images of the chloroplasts were recorded and used to measure plastid area.

Blot hybridization of cpDNA from PFGE

PFGE-separated cpDNA was alkali-denatured, transferred onto a nylon membrane, and neutralized. Procedural details were described previously (Oldenburg and Bendich, 2004b, 2006). An 854 bp fragment of the *Arabidopsis petA* gene was labelled with alkaline phosphatase using AlkPhos Direct Labeling Reagents, and hybridization was detected using the CDP-Star Detection Reagent (GE Healthcare). The hybridization signals were quantified using NIH Image J software (<http://rsb.info.nih.gov/ij/>). Lanes on the image of the blot were selected and the software plotted the intensity of the signal down the lane. The area under the curves generated by the software was calculated to determine the strength of the signal from the corresponding regions of the lanes.

Protein alignment, phylogenetic analysis, and targeting sequence prediction

Protein sequences were obtained from NCBI GenBank (<http://www.ncbi.nlm.nih.gov/sites/entrez?db=nucleotide>), aligned using MacVector™ 8.0 (<http://www.macvector.com/>), and analysed by

the Predotar v. 1.03 (<http://urgi.versailles.inra.fr/predotar.html>) and TargetP 1.1 (<http://www.cbs.dtu.dk/services/TargetP>) targeting sequence prediction algorithms. The coding sequences, also obtained from NCBI GenBank, were aligned using MacClade 4.0.8. (<http://macclade.org/macclade.html>), and a Neighbor-Joining tree was created with these aligned sequences using MEGA 4 (<http://www.megasoftware.net/>) with the default settings.

Results

Organelle-targeted homologues of RecA encoded by the *Arabidopsis* nuclear genome

For two of the three genes encoding chloroplast-targeted RecA proteins of *Arabidopsis*, homozygous T-DNA insertion mutants were obtained by PCR-based genotyping of seeds from SALK T-DNA insertion lines (see Materials and methods). The seeds produced by an individual plant of each genotype (homozygous mutants and their wt counterparts) were collected and the resulting plants were raised to maturity in order to obtain enough seeds to generate sufficient plant tissue for the analysis of cpDNA by PFGE and blot hybridization.

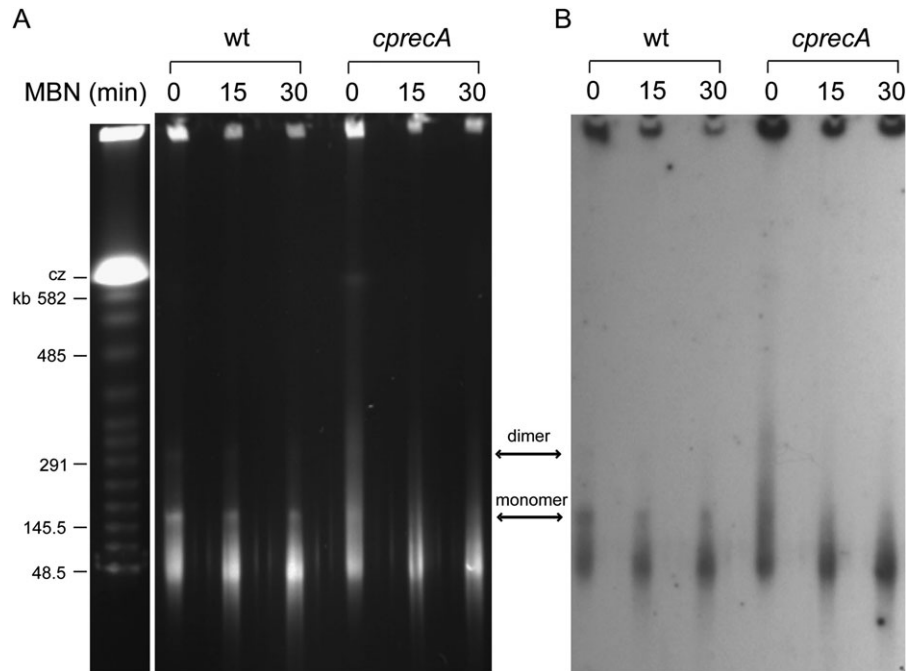


Fig. 4. Detection of single-stranded DNA in wt and *cprecA* mutants. (A) PFGE of cpDNA obtained from an equal volume of pelleted chloroplasts from wt and *cprecA* mutant plants after staining with ethidium bromide. (B) Blot hybridization of the gel in (A) with a *petA* probe. The cpDNA was treated for 0, 15, and 30 min with mung bean nuclease. Linear molecules from *cprecA* mutants show a reduction in size with increasing nuclease treatment. The hybridization signal from the well was half as strong after treatment for 15 min or 30 min for both wt and *cprecA* mutants. Linear DNA sizes (in kb) are indicated. cz, compression zone.

Amount and form of cpDNA in wt and *drt100* mutant plants

At 16 d post-germination, wt and *drt100-1* mutant seedlings had produced 6–7 leaves. For both genotypes, the leaves of the immature plants were <70% of the length reached when fully expanded at maturity. The *drt100-1* mutants appeared morphologically indistinguishable from wt plants. DNA from an equal volume of packed chloroplasts isolated from entire shoots was analysed by PFGE and blot hybridization. For both genotypes, some of the cpDNA remained in the well (Fig. 1, immature). The cpDNA that migrated into the gel was found as linear molecules, including bands at the monomeric, dimeric, and trimeric length of the genome, as well as subgenomic fragments. No band migrating between the well and the compression zone (corresponding to supercoiled circular cpDNA) was observed. The relative amounts and forms of cpDNA did not differ between wt and *drt100* mutant plants, and these results were similar to those for wt plants of several other species (Shaver *et al.*, 2008). The cpDNA from fully expanded third leaves of mature 30-day-old wt and mutant plants (Fig. 1, mature) showed a similar pattern with no evident difference between the two genotypes. However, the amount of cpDNA was reduced ~2-fold in mature plants for both genotypes. Similar results were obtained for plants homozygous for a T-DNA insertion in the middle of the single exon of the *DRT100* gene (*drt100-2*, data not shown). The amount of *DRT100* transcripts was reduced 24-fold in *drt100-1* mutants compared with their wt counterparts as measured

by real-time quantitative PCR (RT-qPCR), and transcripts were essentially undetectable in *drt100-2* mutants (Table 3). It is concluded that severely reducing the RNA level for the *DRT100* gene has no effect on the structure or amount of cpDNA in *Arabidopsis* plants.

Amount and form of cpDNA in wt and *cprecA* mutant plants

The *cprecA* mutants appeared morphologically indistinguishable from wt plants. At 14 d post-germination, the immature seedlings of both wt and *cprecA* mutants had produced six leaves, and all were <70% of the maximum expanded length at maturity. Chloroplasts were isolated from entire shoots and their DNA was analysed by PFGE, blot hybridization, and fluorescence microscopy. Well-bound cpDNA and the genomic monomer and dimer were detected with wt plants, but the cpDNA of the *cprecA* mutants did not show prominent bands at the size of the monomer or dimer. Only the well-bound cpDNA and a smear of linear DNA molecules from ~40 kb to 500 kb were evident, and the hybridization signal was only 60% as intense as the signal from DNA obtained from an equal volume of wt chloroplasts (Fig. 2A, B, immature). Linear forms of cpDNA from fully-expanded first and second leaves of mature 23-day-old wt and *cprecA* mutant plants were not detected, even after a longer exposure (not shown), probably because the amount of DNA from chloroplasts of mature plants was 3- to 6-fold lower than that from an equal volume of chloroplasts from immature plants (Fig. 2A, B,

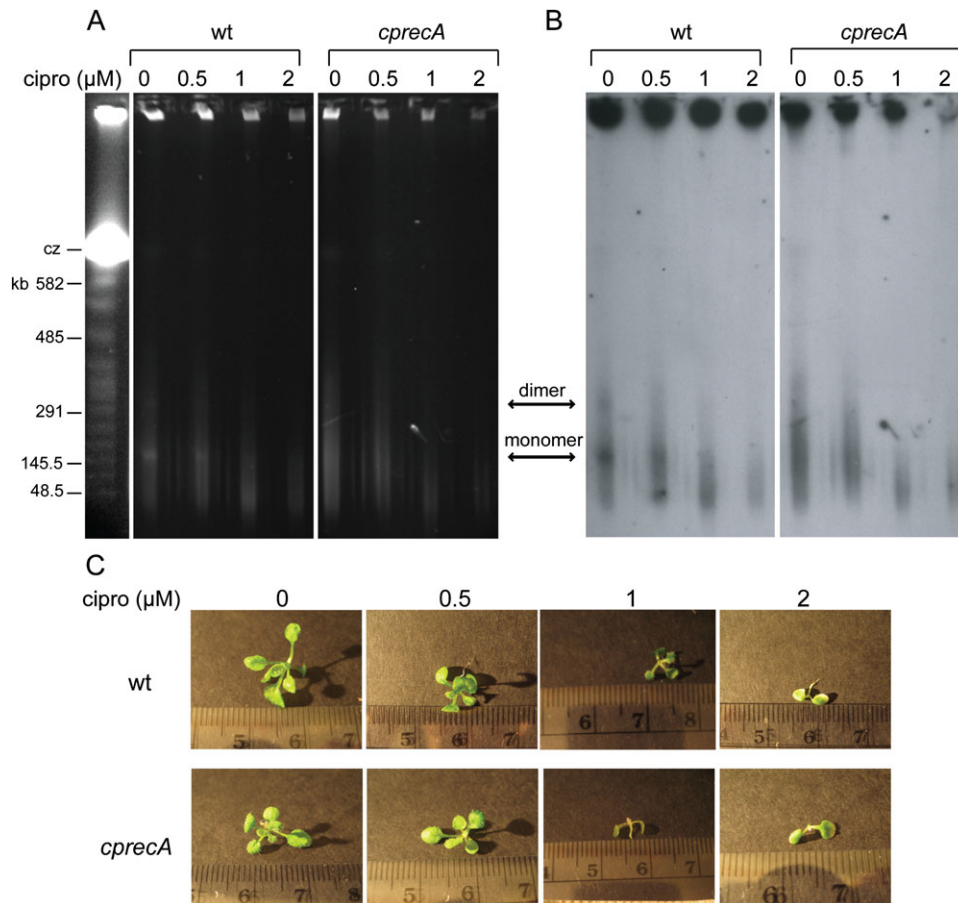


Fig. 5. Structure of cpDNA in wt and *cprecA* mutants after treatment with ciprofloxacin. (A) PFGE of cpDNA obtained from an equal volume of pelleted chloroplasts from wt and *cprecA* mutant plants after staining with ethidium bromide. (B) Blot hybridization of the gel in (A) with a *petA* probe. Plants were grown for 14 d on 0, 0.5, 1, and 2 μM ciprofloxacin. Ciprofloxacin-induced DSBs lead to loss of monomers and dimers in wt plants, similar to *cprecA* mutants without ciprofloxacin. Ciprofloxacin leads to a reduction in the size of the DNA that migrates as a smear in *cprecA* mutants. Linear DNA sizes (in kb) are indicated. cz, compression zone. (C) Representative images of wt and *cprecA* mutant plants after 14 d on 0, 0.5, 1, and 2 μM ciprofloxacin. The small gradations are millimetres. Increasing ciprofloxacin treatment leads to reduced growth in both wt and *cprecA* mutant plants.

mature). The *cpRecA* transcript level was only 15% of the wt level as determined by RT-qPCR (Table 3). Individual chloroplasts from immature *cprecA* mutant plants contained ~ 2 -fold fewer genome equivalents on average compared with their wt counterparts (Fig. 2C). For mature leaves, the amount of DNA per chloroplast did not differ between wt and *cprecA* mutants (Fig. 2D). It is concluded that the *cpRecA* gene has a role in maintaining the structure of cpDNA molecules and the amount of DNA retained in immature chloroplasts.

Amount and form of cpDNA in *cprecA drt100-1* mutant plants

It is possible that *cpRecA* exhibits functional redundancy with *DRT100*, allowing *cpRecA* to compensate for the loss of *DRT100* function in *drt100* mutant plants. To examine this possibility, the cpDNA of *cprecA drt100-1* double mutants was analysed. If these genes have partially overlapping functions, the phenotype of the double mutants is expected to differ from that of the single mutants. F_1 seeds

from the cross *cprecA* \times *drt100-1* were allowed to self, generating a segregating F_2 population. Two *cprecA drt100-1* individuals and one wt plant isolated from this population were allowed to self. Progeny seeds from these plants and from an independent wt strain (Col) were grown for 13 d. All of these immature plants appeared visually indistinguishable and had produced six leaves; each was $< 70\%$ of its final expanded length. Chloroplasts were isolated from entire shoots and the cpDNA was analysed by PFGE. The forms of cpDNA for both wt siblings of the double mutants and the independent wt strain consisted of both well-bound cpDNA and migrating linear forms, including bands at the positions of the monomer and dimer (Fig. 3). In contrast, both of the *drt100-1 cprecA* lines showed a phenotype that was similar to that of the *cprecA* single mutant: linear forms of DNA migrating as a smear of fragments ranging in size from ~ 40 kb to 500 kb with no prominent bands. Double mutants generated using a reciprocal cross (*drt100-2* \times *cprecA*) gave the same result (data not shown). If *DRT100* and *cpRecA* acted redundantly, the cpDNA phenotype of double mutants is expected to differ

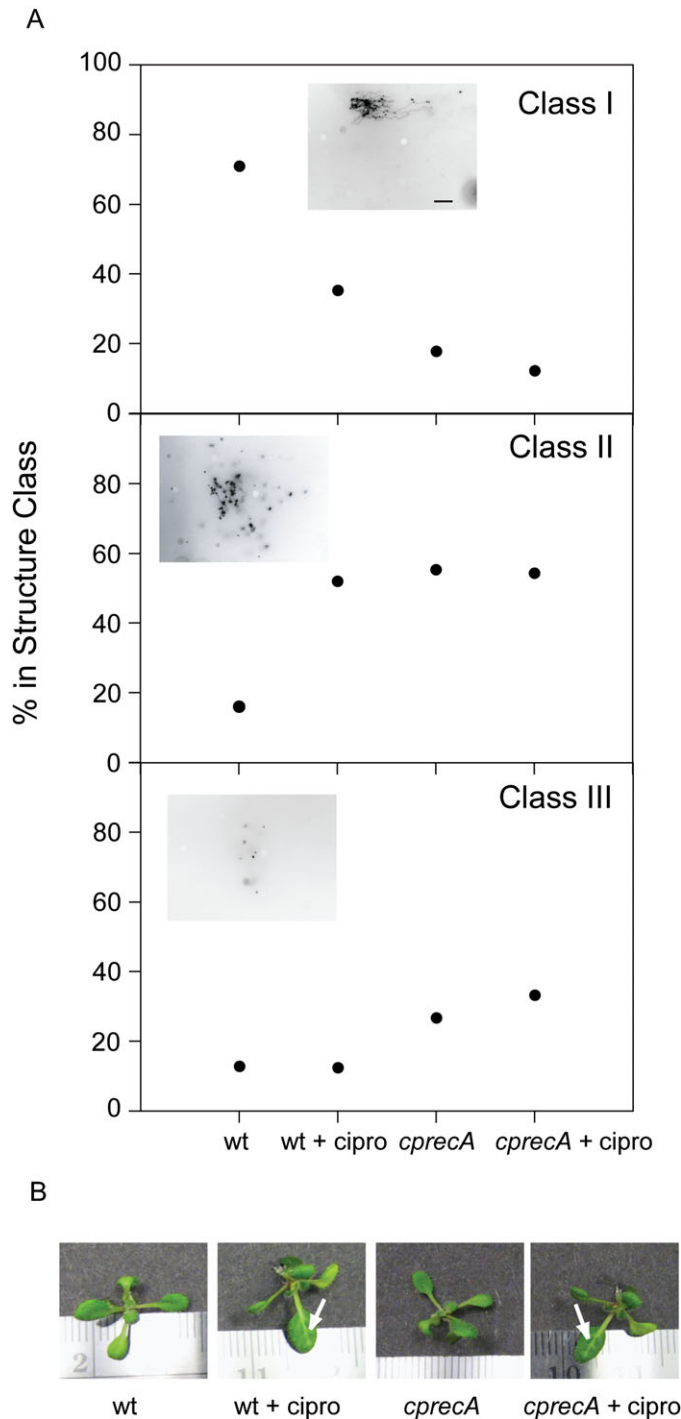


Fig. 6. Comparison of the structural forms of individual cpDNA molecules in wt and *cprecA* plants after ciprofloxacin treatment. Wt and *cprecA* plants after 11 d of growth followed by 3 d of treatment with water or 30 μ M ciprofloxacin. (A) Deproteinized cpDNA was stained with ethidium bromide, visualized by fluorescence microscopy, and characterized by structural class. Class I structures, complex forms consisting of a network of connected fibres or fibres connected to a large, dense core; class II structures, complex forms with a greater number of unconnected fibres than connected fibres; class III structures, unconnected fibres without a complex form. Representative images of class I, II, and III molecules are shown in the insets. The small dots in the

from the phenotype of either single mutant. The double mutant phenotype did not differ from that of the *cprecA* single mutant. Thus, these genes do not act redundantly.

Single-stranded cpDNA in wt and *cprecA* mutants

In *E. coli*, RecA is involved in the repair of single-stranded gaps and DSBs (Michel *et al.*, 2007). During the repair of DSBs, single-stranded DNA (ssDNA) is produced through the exonucleolytic action of the RecBCD protein (Kowalczykowski, 2000). The RecA protein binds along the single-stranded regions and facilitates repair by homologous recombination, while preventing more extensive exonuclease activity (Skarstad and Boye, 1993). Thus, it might be expected that a reduction in RecA activity would result in more ssDNA. Wt and *cprecA* cpDNA (from 14-day-old seedling shoots) were treated with mung bean nuclease [an enzyme with endonuclease activity on single-strand gaps in double-stranded DNA (dsDNA) and 5' to 3' exonuclease activity on ssDNA (Kroeker and Kowalski, 1978)] for 15 min or 30 min or left the DNA untreated. Linear genomic oligomers of wt cpDNA were unaffected by treatment with this nuclease (Fig. 4). However, the amount of well-bound cpDNA decreased after treatment with mung bean nuclease. This result indicates that the well-bound form of cpDNA contains single-stranded regions, whereas the linear genomic oligomers consist primarily of dsDNA. An increase in the smear of subgenomic fragments smaller than 50 kb is also apparent after digestion with mung bean nuclease. These fragments may arise from cpDNA that has been liberated from the well. Thus, the replicating forms of cpDNA from young wt plants may consist of single-stranded regions interspersed with dsDNA at intervals of <50 kb.

After treatment with mung bean nuclease, *cprecA* mutants exhibited a decrease in both the hybridization signal from the well-bound cpDNA and the range of sizes of the linear forms of cpDNA. Thus, all of the forms of cpDNA in the *cprecA* mutants contain single-stranded regions, but only the well-bound cpDNA in wt contains ssDNA detectable with this enzyme, suggesting that cpRecA and *E. coli* RecA may act similarly.

images are shorter fibres of DNA that remained condensed during preparation for fluorescence microscopy. The scale bar in the class I image is 10 μ m and applies to all images in (A). The number of molecules examined for wt, wt+cipro, *cprecA*, and *cprecA*+cipro was 62, 48, 56, and 57, respectively. No circular forms were observed among these 223 molecules. A chi-squares test of independence showed that the distributions of molecules among classes I–III for wt+cipro, *cprecA*, and *cprecA*+cipro differed from the wt ($P < 0.001$). (B) Representative images of wt and *cprecA* plants after treatment with ciprofloxacin. Treatment with ciprofloxacin caused bleaching along the vasculature of older leaves of both wt and *cprecA* mutant plants. Arrows indicate bleaching along the vasculature. The small gradations are millimetres.

Table 2. Primers used for PCR genotyping and RT-qPCR

Product	Forward primer	Reverse primer
Genotyping		
<i>drt100-1</i>	CTGATATTTCTCTCCGGGGAG (wt) or LBb1 (<i>drt100-1</i>)	TACCTGTCCGTTGCCAGTAAC
<i>drt100-2</i>	GATACCATGCACATGCAAATG (wt) or LBb1 (<i>drt100-2</i>)	GGGTATAGTTCCTTCCAAGCGC
<i>cprecA</i>	TAGGGTGAGATTGGAATGCAG (wt) or LBb1 (<i>cprecA</i>)	AAGAGCTGCTGCTCATCAAAG
LBb1	GCGTGGACCGCTTGCTGCAACT	
RT-qPCR		
<i>DRT100</i>	GCACTCACTTCCCTCGTTCT	TTTCCGAGAGTTTGCCGATTT
<i>cpRecA</i>	CAGAGGTGACTAGCGGAGGA	ACTCTTACACGAGCCCCGAAG
<i>ACT2</i>	GCCATCCAAGCTGTTCTCTC	GCTCGTAGTCAACAGCAACAA

Double-strand cpDNA breaks in wt and *cprecA* mutants

It is possible that the extensive smear of linear cpDNA fragments in *cprecA* mutants is due to a lack of DNA damage repair. Thus, *cprecA* mutant plants would be especially vulnerable to agents that damage DNA. Also, some types of DNA damage, such as DSB, in wt plants would be expected to produce a similar cpDNA phenotype to that in *cprecA* mutants. Ciprofloxacin is a type II topoisomerase inhibitor that induces DSBs during DNA replication in prokaryotes, but not in the eukaryotic nucleus (Jacoby, 2005), and has been shown to affect chloroplasts in *Arabidopsis* (Wall *et al.*, 2004). The nuclear genome of *Arabidopsis* encodes organelle-targeted type II topoisomerases homologous to bacterial gyrase: a GyrA subunit that is targeted to both mitochondria and chloroplasts, one GyrB subunit that is targeted to mitochondria only, and one GyrB subunit that is targeted to chloroplasts only (Wall *et al.*, 2004). Wt and *cprecA* plants grown on agar plates containing 0, 0.5, 1, or 2 μM ciprofloxacin were investigated.

The immature, 14-day-old wt seedlings grown without ciprofloxacin had produced 6–7 rosette leaves and all were <70% of their final size (Fig. 5C). After 14 d of growth in 0.5 μM ciprofloxacin, wt seedlings had a more compact rosette and produced 5–6 leaves, but appeared otherwise similar to the control plants grown without ciprofloxacin. Plants grown in 1 μM ciprofloxacin appeared slightly chlorotic and produced only two rosette leaves; and those in 2 μM ciprofloxacin appeared extremely chlorotic and produced no rosette leaves. The *cprecA* plants appeared similar to wild-type plants for all growth conditions except 1 μM ciprofloxacin. Under this condition, *cprecA* mutants appeared more chlorotic and had smaller rosette leaves than the wt. Thus, a dose-dependent effect of ciprofloxacin on seedling morphology is found for both the wt and *cprecA*. The effect, however, is more pronounced for the *cprecA* mutant.

For wt plants, growth in 0.5 μM ciprofloxacin resulted in a less distinct monomer band and no DNA band at the dimer position (Fig. 5B). The monomer band was completely absent in wt plants grown in 1 μM or 2 μM ciprofloxacin. The size range of the smear of cpDNA fragments for *cprecA* plants became smaller with increasing concentrations of ciprofloxacin. The decrease in prevalence of the oligomeric bands (and decline in the amount of well-bound DNA) with increasing concentrations of ciprofloxacin for the wt plants

Table 3. mRNA for *DRT100* and *cpRecA* in wt and T-DNA mutants

The levels of mRNA for *DRT100* and *cpRecA* were determined relative to the actin gene *ACT2*. The highest level for each gene was assigned a value of 1 and all other levels are relative to that value. A very small value for the expression level of *DRT100* in *drt100-2* plants was rounded to two decimal places, resulting in 0.00.

Genotype	<i>DRT100</i> transcripts	<i>cpRecA</i> transcripts
Wt ^a	0.81±0.08	
Wt ^b	1.00±0.07	
Wt ^c		1.00±0.10
<i>drt100-1</i>	0.03±0.00	
<i>drt100-2</i>	0.00±0.00	
<i>cprecA</i>		0.15±0.03

^a Wt plants from the T-DNA insertion line for the *drt100-1* allele.

^b Wt plants from the T-DNA insertion line for the *drt100-2* allele.

^c Wt plants from the T-DNA insertion line for the *cprecA* allele.

probably reflects an increase in DSBs caused by ciprofloxacin-mediated inhibition of type II topoisomerase activity (Jacoby, 2005). Similarly, the decrease in the monomeric and dimeric bands and increase in the smear of linear DNA for the *cprecA* mutants would be due to an increase in DSBs without repair.

In order to characterize further the effect of the *cprecA* mutation and cpDNA damage on cpDNA structure, individual cpDNA molecules were examined using fluorescence microscopy of deproteinized cpDNA stained with ethidium bromide. After 11 d of growth, wt and *cprecA* plants were either mock treated (with water) or treated with 30 μM ciprofloxacin and allowed to grow for a further 3 d. Plants that were treated with ciprofloxacin showed bleaching along the vasculature of leaves that were produced before the treatment with the drug (Fig. 6B, white arrows). The basal halves of the leaves that were produced after the treatment were entirely bleached. Figure 6A shows that most (71%) of the cpDNA images from mock-treated wt plants were found as class I forms (complex, multigenomic, branched linear structures with more DNA fibres connected to a core than unconnected fibres). Class II forms (complex structures with more unconnected DNA fibres than fibres connected to a core) made up 16% and class III (no complex structures; only unconnected DNA fibres) made

up only 13% of the forms of cpDNA. After treatment with ciprofloxacin, the proportion of class I forms decreased to 35%, and there was a corresponding increase in the proportion of class II forms (52%) but no increase in class III forms. Class I represented only 18% of all forms in mock-treated *cprecA* mutants, with most of the cpDNA found in class II (55%) and class III (27%). After treatment with ciprofloxacin, there was only a minor decrease in the proportion of class I (13%) and a minor increase in the proportion of class III (33%). It is surmised that ciprofloxacin-induced DSBs cause a conversion from class I to class II forms in wt plants. The unconnected fibres seen in classes II and III appear as simple linear molecules that would migrate in the smear of cpDNA during PFGE, whereas the complex branched forms remain immobile in the well of the gel (Oldenburg and Bendich, 2004b). Both assay procedures used to assess molecular integrity (Figs. 2–6) show that the molecules of cpDNA from *cprecA* mutant plants are more fragmented than those of wt plants.

Phenotypic effects after growth of *cprecA* mutants for multiple generations

None of the *cprecA* mutants from the first three generations of selfing showed any abnormal visible phenotype. During the next four generations, however, *cprecA* mutants exhibited a range of visible phenotypes (Fig. 7). The most common was colour variegation in leaf sectors. Tissue necrosis in mature leaves was also observed. The percentage of plants exhibiting a phenotype varied from 1.1% to 4.2% and did not increase with each successive generation (Table 4). Additional unlinked inserts in the genomes of these mutants might be responsible for the phenotypes observed. This possibility, however, is unlikely because none of the wt plants isolated from the same T-DNA insertion line exhibited an abnormal phenotype in seven generations, suggesting that the phenotypes observed in the *cprecA* mutants are caused by disruption of the *cprecA* gene. It is possible, however, that additional T-DNA insertions very tightly linked to the insertion in *cpRecA* may be present in this line. PCR was used to determine whether any of the 13 genes in the region from 25 kb upstream to 25 kb downstream of *cprecA* contained an insertion (Supplementary Table S1 available at *JXB* online). For each gene, two individual plants were examined from different generations that either contained or did not contain the insert in *cpRecA*. No inserts were found in the genes in the 50 kb region surrounding *cpRecA*. It is concluded that the T-DNA disruption of the *cpRecA* gene is responsible for the phenotypes observed.

Discussion

There is a dearth of information about repair of DNA in chloroplasts. Two *Arabidopsis* nuclear genes predicted to encode chloroplast-targeted proteins that are similar to bacterial RecA were investigated. Impairing the function of

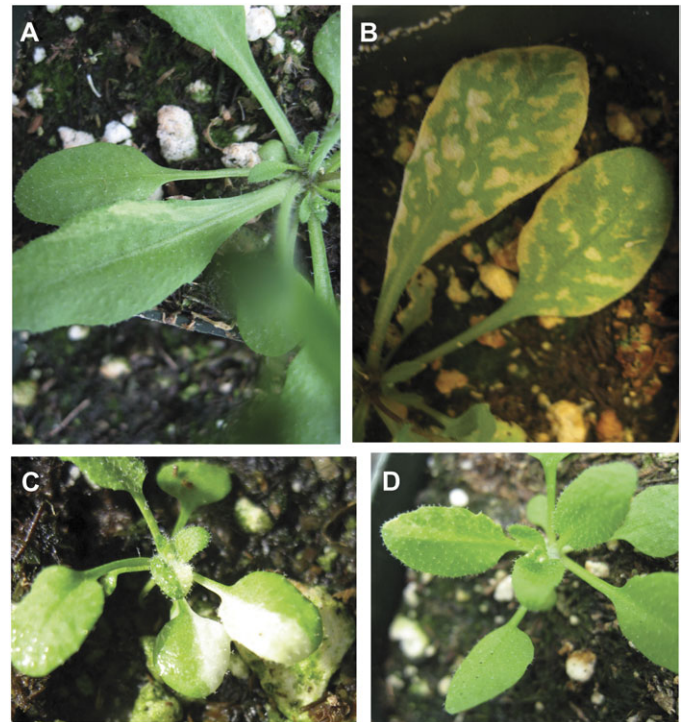


Fig. 7. Phenotypes of *cprecA* mutants. Representative images of four *cprecA* mutant phenotypes. (A) Green and white variegated sectors. (B) Necrosis of tissue farthest from vasculature. (C) Albino sectors. (D) Green and yellow variegated sectors. Since none of the wt plants derived from the T-DNA insertion line exhibited an abnormal phenotype after seven generations, the abnormal phenotypes of *cprecA* mutants can be attributed to T-DNA disruption of the *cpRecA* gene and not to additional T-DNA insertions that may be present in this line.

Table 4. Phenotypes of *cprecA* mutants after several generations of growth

Generation	No. of plants examined	Percentage with phenotype ^a
4 ^b	36	2.8
5	72	4.2
6	210	1.4
7	177	1.1

^a Phenotypes scored were colour variegation and tissue necrosis.

^b No phenotypic abnormality was observed among several hundred *cprecA* mutant plants during the first three generations or among wt plants after seven generations.

one of these genes, *cpRecA*, led to abnormalities in both cpDNA and plant morphology. Although chloroplast-targeted *E. coli* RecA homologues have been implicated in cpDNA maintenance and repair (Cerutti *et al.*, 1992, 1993, 1995; Pang *et al.*, 1992; Cao *et al.*, 1997; Inouye *et al.*, 2008), the results provide the first evidence that homologous recombination is used to maintain the structural integrity of DNA molecules in the chloroplasts of vascular plants.

A mutation in the other gene, *DRT100*, had no apparent effect and did not act redundantly with *cpRecA*. The amino acid sequence of the DRT100 protein differs considerably from that of bacterial RecA and other nuclear-encoded, organelle-targeted RecA proteins (Supplementary Fig. S1 at *JXB* online). Pang *et al.* (1992) reported that this protein had a chloroplast localization signal. Two current signal peptide prediction algorithms, TargetP and Predotar, both predict that this protein is targeted to the secretory pathway (see Materials and methods). Although *DRT100* can complement *recA* mutants of *E. coli* (Pang *et al.*, 1992), it may not function as a RecA protein in chloroplasts.

Abnormal cpDNA molecules in *cprecA* mutants

In PFGE, the cpDNA from wt plants and *drt100* mutants was found as well-bound and as a smear of migrating linear forms, including discrete bands representing the genomic monomer, dimer, and trimer. The well-bound cpDNA is partially single stranded, consistent with an earlier proposal that the DNA that remains in the well is a branched form of replicating DNA that serves as the segregating genetic unit, the chromosome, in both chloroplasts (Oldenburg and Bendich, 2004a, b) and mitochondria (Oldenburg and Bendich, 1996). The molecular integrity of the branched cpDNA was greatly reduced in the *cprecA* mutants, as it was in wt plants treated with the prokaryotic type II topoisomerase inhibitor ciprofloxacin (Fig. 6A). Fragmentation of the cpDNA molecules in *cprecA* mutants increased only slightly after treatment with ciprofloxacin. If cpDNA replication occurs through a recombination-dependent mechanism (Oldenburg and Bendich, 2004a, b), cpDNA replication might be compromised in *cprecA* mutants. If so, fewer topoisomerase–DNA complexes would be expected for the cpDNA of *cprecA* mutants, leading to fewer instances of DSBs generated by ciprofloxacin-mediated suppression of topoisomerase activity.

During PFGE, the migrating cpDNA of *cprecA* mutants appeared as a smear of linear fragments without any distinct bands (Fig. 2). Prominent linear genomic monomers and oligomers of cpDNA have been observed for many wt plant species, including maize (*Zea mays*; Oldenburg and Bendich, 2004a, b; Oldenburg *et al.*, 2006), *Medicago truncatula* (Shaver *et al.*, 2006, 2008), wheat (*Triticum aestivum*; Shaver *et al.*, 2006), *Chenopodium album* (Backert *et al.*, 1995), tobacco (*Nicotiana tabacum*; Backert *et al.*, 1995; Lilly *et al.*, 2001; Scharff and Koop, 2006), pea (*Pisum sativum*; Bendich and Smith, 1990; Lilly *et al.*, 2001), watermelon (*Citrullus vulgaris*; Bendich and Smith, 1990), spinach (*Spinacia oleracea*; Deng *et al.*, 1989), and *Marchantia polymorpha* (Oldenburg and Bendich, 1998). Thus, it is likely that the cpDNA repair process has been conserved among plants and maintains linear monomeric and oligomeric forms of cpDNA. The lack of such monomers and oligomers in *cprecA* mutants may result from the failure either to repair DSBs or to produce telomeric ends that prevent degradation of such linear DNA molecules within the plastid. Homologous recombination has been suggested

as a telomerase-independent mechanism for maintenance of eukaryotic telomeres (Tarsounas and West, 2005; Raji and Hartsuiker, 2006) and may similarly protect the ends of linear cpDNA molecules even though the structures of linear cpDNA ends and eukaryotic telomeres differ.

It might seem surprising that ciprofloxacin did not have a more substantial impact on the growth or morphology of *cprecA* mutants than wt plants. On the other hand, cpDNA may be present in excess, so that morphological effects may go undetected until most of the cpDNA is damaged. Additionally, DSBs generated by ciprofloxacin remain in a complex with topoisomerase (Chen *et al.*, 1996) and may not act as substrates for repair by RecA. Furthermore, the additional chloroplast-targeted RecA protein (RECA2; AT2G19490) may partially complement the *cprecA* mutation.

Delayed phenotype of *cprecA* mutants

It is demonstrated that a recombinational repair system is required for the stability of the chloroplast chromosome. After several generations of selfing, the *cprecA* mutants exhibited visible phenotypes, including tissue necrosis and colour variegation among leaf sectors. Why was the morphological consequence of cpDNA damage apparent only after several generations? One reason follows from the non-Mendelian nature of organellar inheritance and another from analogy to recombination-dependent DNA repair in *E. coli*.

It may have taken several generations to generate sectors of cells containing chloroplasts in which most of the DNA is damaged or degraded, given the stochastic partitioning of damaged and wt chloroplast chromosomes during chloroplast division and the stochastic partitioning of chloroplasts during cell division (Birky, 2001). Many animals experience a lifetime accumulation of mtDNA damage, which varies among cells in different tissues and organs (Trifunovic and Larsson, 2008; Kukat and Trifunovic, 2009). Variation in mtDNA damage among cells may reflect differential efficiency of mtDNA repair among tissues (Gredilla *et al.*, 2008). Impairment of mitochondrial function due to accumulated mtDNA mutations is proposed to contribute to ageing. Decline of respiratory function may result from random partitioning of normal and damaged mtDNA molecules during cell division, leading to clonal expansion of cells with damaged mtDNA (Nagley *et al.*, 1992; Trifunovic and Larsson, 2008). As it takes many cell generations to observe the phenotypic consequences of mtDNA damage during ageing in animals, it may similarly require many cell generations for the consequences of cpDNA damage in *cprecA* mutants to become evident. Another possibility is that the degradation of cpDNA with damaged ends occurs rather slowly. In *E. coli*, RecA-dependent recombination involves the RecBCD exonuclease, which is maintained at a low concentration (~10 enzyme complexes per cell) in order to prevent unintentional degradation of the *E. coli* chromosome (Dillingham and Kowalczykowski, 2008). The functional analogue of the RecBCD complex for *Arabidopsis* chloroplasts (which is not yet known) may similarly be maintained

at a low concentration, leading to a gradual degradation of cpDNA molecules when *cpRecA* activity is impaired.

Visible phenotypes due to chloroplast chromosome instability might be expected to increase in frequency with each successive generation. Instability of the nuclear genome due to telomerase deficiency results in increasingly deleterious phenotypes with successive generations in *Arabidopsis* and mouse (Lee *et al.*, 1998; Riha *et al.*, 2001). However, the percentage of *cprecA* mutant plants with observable phenotypes of *cprecA* mutants varied from 1.1% to 4.2% but with no generational increase. One explanation for this surprising observation is that additional repair processes might be activated after several generations without functional *cprecA*. For example, non-homologous end-joining (a mechanism not yet known for cpDNA repair) is used as an alternative to homologous recombination for DSB repair in both prokaryotes and eukaryotes (Pitcher *et al.*, 2007). RECA2 is targeted to both mitochondria and chloroplasts, might be partially functionally redundant with *cprecA*, and might compensate for the lack of *cprecA* activity. Another possibility is that the chloroplast chromosomes that are transmitted to the next generation might sustain less damage than cpDNA in green cells because gametes originate from meristematic cells where photosynthesis [a major source of DNA-damaging reactive oxygen species (Roldan-Arjona and Ariza, 2009)] does not occur.

The *chloroplast mutator* of barley leads to cytoplasmically inherited chlorophyll deficiencies (Prina, 1992), one of which is due to point mutations in the chloroplast *infA* gene (Landau *et al.*, 2007), suggesting that the *chloroplast mutator* gene may be responsible for cpDNA repair in barley. The chloroplast mutator (*CHM*) of *Arabidopsis* was originally identified as a nuclear mutation affecting maintenance of cpDNA (Redei and Plurad, 1973) and is now recognized as a homologue of the *E. coli* mismatch repair gene, *MutS*. Although *CHM* (renamed *MSH1*) is targeted to both mitochondria and chloroplasts, only the mitochondrial genome is affected in *chm* mutants (Martinez-Zapater *et al.*, 1992; Sakamoto *et al.*, 1996; Shedge *et al.*, 2007). A recent study identifies a function for the Whirly proteins (ssDNA-binding proteins) in stabilizing the chloroplast genomes of *A. thaliana* and *Z. mays* (Marechal *et al.*, 2009). For *Arabidopsis*, the authors report variegated phenotypes arising in 4.6% of *AtWhy1* and *AtWhy3* double knockout plants due to illegitimate recombination. Many *Arabidopsis* variegation mutants have not yet been characterized (Yu *et al.*, 2007). Future research on these proteins and RECA2 will shed light on the spectrum of repair processes for cpDNA.

In conclusion, the *cpRecA* gene maintains the integrity of cpDNA, possibly through repair of DSBs or maintenance of telomere-like ends of linear molecules. The phenotypic abnormalities that arise after multiple generations are reminiscent of the ageing phenotypes attributed to declining mitochondrial function in yeast and animals (Mandavilli *et al.*, 2002), an interesting parallel considering that the mitochondrion-targeted *RecA* homologue was lost in the common ancestor of yeast and animals (Lin *et al.*, 2006).

Accession numbers

Arabidopsis Genome Initiative (AGI) locus identifiers for the *RecA* homologues described in this article are listed in Table 1. The *Arabidopsis* Information Resource (TAIR) accession numbers are 2091260 for *DRT100* and 2207445 for *cpRecA*.

Supplementary data

Supplementary data are available at *JXB* online.

Supplementary Table S1. PCR-based detection of insertions in 13 genes in the 50 kb region surrounding *cpRecA*. The primers were used to amplify DNA from at least two individuals from two different generations with or without the insertion in *cpRecA*. If the gene was larger than 1 kb, then overlapping sets of primers were used to span the entire length of the gene (indicated in the table after the name of the gene as “s1, s2, etc.”). N indicates that no inserts were detected. The primers were used to amplify DNA from at least two individuals from two different generations with or without the insertion in *cpRecA*. If the gene was larger than 1 kb, then overlapping sets of primers were used to span the entire length of the gene (indicated in the table after the name of the gene as “s1, s2, etc.”). N indicates that no inserts were detected.

Fig. S1. Protein alignment and phylogeny of coding regions of putative *RecA* homologues. (A) Protein alignment for *cpRecA* and three other *RecA* homologues (*DRT100*, *AT2G19490*, and *AT3G10140*) encoded in the *Arabidopsis* nuclear genome, *Chlamydomonas reinhardtii* (*C. reinhardtii*, nuclear-encoded, chloroplast-targeted homologue), *Synechococcus elongatus* (*S. elongatus*, cyanobacterial homologue), and *E. coli* *RecA*. The last line shows the consensus sequence. (B) Neighbor-Joining tree of coding sequences (excluding the region coding for the signal peptide). Values at nodes are bootstrap values from 20 000 replicates.

Acknowledgements

We thank Amanda Rychel for assistance with the phylogenetic analysis of *RecA* sequences, and Jennifer Nemhauser and the Comparative Genomics Center at the University of Washington for material support. This investigation was supported in part by Public Health Service National Research Award T32 GM07270 from the National Institute of General Medical Sciences and by the Frye-Hotson-Rigg fellowship from the University of Washington Department of Biology.

References

- Aguilera A, Gomez-Gonzalez B. 2008. Genome instability: a mechanistic view of its causes and consequences. *Nature Reviews Genetics* **9**, 204–217.

- Backert S, Dorfel P, Börner T.** 1995. Investigation of plant organellar DNAs by pulsed-field gel electrophoresis. *Current Genetics* **28**, 390–399.
- Bendich AJ, Smith SB.** 1990. Moving pictures and pulsed-field gel electrophoresis show linear DNA molecules from chloroplasts and mitochondria. *Current Genetics* **17**, 421–425.
- Birky Jr CW.** 2001. The inheritance of genes in mitochondria and chloroplasts: laws, mechanisms, and models. *Annual Review of Genetics* **35**, 125–148.
- Bohr VA, Anson RM.** 1999. Mitochondrial DNA repair pathways. *Journal of Bioenergetics and Biomembranes* **31**, 391–398.
- Cao J, Combs C, Jagendorf AT.** 1997. The chloroplast-located homolog of bacterial DNA recombinase. *Plant and Cell Physiology* **38**, 1319–1325.
- Cerutti H, Ibrahim HZ, Jagendorf AT.** 1993. Treatment of pea (*Pisum sativum* L.) protoplasts with DNA-damaging agents induces a 39-kilodalton chloroplast protein immunologically related to *Escherichia coli* RecA. *Plant Physiology* **102**, 155–163.
- Cerutti H, Johnson AM, Boynton JE, Gillham NW.** 1995. Inhibition of chloroplast DNA recombination and repair by dominant negative mutants of *Escherichia coli* RecA. *Molecular and Cellular Biology* **15**, 3003–3011.
- Cerutti H, Osman M, Grandoni P, Jagendorf AT.** 1992. A homolog of *Escherichia coli* RecA protein in plastids of higher plants. *Proceedings of the National Academy of Sciences, USA* **89**, 8068–8072.
- Chen CR, Malik M, Snyder M, Drica K.** 1996. DNA gyrase and topoisomerase IV on the bacterial chromosome: quinolone-induced DNA cleavage. *Journal of Molecular Biology* **258**, 627–637.
- Cox MM.** 2007. Regulation of bacterial RecA protein function. *Critical Reviews in Biochemistry and Molecular Biology* **42**, 41–63.
- Deng XW, Wing RA, Gruissem W.** 1989. The chloroplast genome exists in multimeric forms. *Proceedings of the National Academy of Sciences, USA* **86**, 4156–4160.
- Dillingham MS, Kowalczykowski SC.** 2008. RecBCD enzyme and the repair of double-stranded DNA breaks. *Microbiology and Molecular Biology Reviews* **72**, 642–671.
- Gredilla R, Garm C, Holm R, Bohr VA, Stevnsner T.** 2008. Differential age-related changes in mitochondrial DNA repair activities in mouse brain regions. *Neurobiology of Aging* doi:10.1016/j.neurobiolaging.2008.07.004.
- Inouye T, Odahara M, Fujita T, Hasebe M, Sekine Y.** 2008. Expression and complementation analyses of a chloroplast-localized homolog of bacterial RecA in the moss *Physcomitrella patens*. *Biosciences, Biotechnology and Biochemistry* **72**, 1340–1347.
- Jacoby GA.** 2005. Mechanisms of resistance to quinolones. *Clinical Infectious Diseases* **41**, S120–S126.
- Khazi FR, Edmondson AC, Nielsen BL.** 2003. An *Arabidopsis* homologue of bacterial RecA that complements an *E. coli* recA deletion is targeted to plant mitochondria. *Molecular Genetics and Genomics* **269**, 454–463.
- Kimura S, Sakaguchi K.** 2006. DNA repair in plants. *Chemical Reviews* **106**, 753–766.
- Kowalczykowski SC.** 2000. Initiation of genetic recombination and recombination-dependent replication. *Trends in Biochemical Sciences* **25**, 156–165.
- Kroeker WD, Kowalski D.** 1978. Gene-sized pieces produced by digestion of linear duplex DNA with mung bean nuclease. *Biochemistry* **17**, 3236–3243.
- Kukat A, Trifunovic A.** 2009. Somatic mtDNA mutations and aging—facts and fancies. *Experimental Gerontology* **44**, 101–105.
- Landau A, Diaz Paleo A, Civitillo R, Jaureguiualzo M, Prina AR.** 2007. Two infA gene mutations independently originated from a mutator genotype in barley. *Journal of Heredity* **98**, 272–276.
- Lee HW, Blasco MA, Gottlieb GJ, Horner 2nd JW, Greider CW, DePinho RA.** 1998. Essential role of mouse telomerase in highly proliferative organs. *Nature* **392**, 569–574.
- Li X, Heyer WD.** 2008. Homologous recombination in DNA repair and DNA damage tolerance. *Cell Research* **18**, 99–113.
- Lilly JW, Havey MJ, Jackson SA, Jiang J.** 2001. Cytogenomic analyses reveal the structural plasticity of the chloroplast genome in higher plants. *The Plant Cell* **13**, 245–254.
- Lin Z, Kong H, Nei M, Ma H.** 2006. Origins and evolution of the recA/RAD51 gene family: evidence for ancient gene duplication and endosymbiotic gene transfer. *Proceedings of the National Academy of Sciences, USA* **103**, 10328–10333.
- Livak KJ, Schmittgen TD.** 2001. Analysis of relative gene expression data using real-time quantitative PCR and the 2⁻(Delta Delta C(T)) method. *Methods* **25**, 402–408.
- Mandavilli BS, Santos JH, Van Houten B.** 2002. Mitochondrial DNA repair and aging. *Mutation Research* **509**, 127–151.
- Marechal A, Parent JS, Veronneau-Lafortune F, Joyeux A, Lang BF, Brisson N.** 2009. Whirly proteins maintain plastid genome stability in *Arabidopsis*. *Proceedings of the National Academy of Sciences, USA* **106**, 14693–14698.
- Martinez-Zapater JM, Gil P, Capel J, Somerville CR.** 1992. Mutations at the *Arabidopsis* CHM locus promote rearrangements of the mitochondrial genome. *The Plant Cell* **4**, 889–899.
- Michel B, Boubakri H, Baharoglu Z, LeMasson M, Lestini R.** 2007. Recombination proteins and rescue of arrested replication forks. *DNA Repair* **6**, 967–980.
- Murashige T, Skoog F.** 1962. A revised medium for rapid growth and bioassay with tobacco tissue culture. *Physiologia Plantarum* **15**, 473–497.
- Nagley P, Mackay IR, Baumer A, Maxwell RJ, Vaillant F, Wang ZX, Zhang C, Linnane AW.** 1992. Mitochondrial DNA mutation associated with aging and degenerative disease. *Annals of the New York Academy of Sciences* **673**, 92–102.
- Nakazato E, Fukuzawa H, Tabata S, Takahashi H, Tanaka K.** 2003. Identification and expression analysis of cDNA encoding a chloroplast recombination protein REC1, the chloroplast RecA homologue in *Chlamydomonas reinhardtii*. *Biosciences, Biotechnology and Biochemistry* **67**, 2608–2613.
- Niedernhofer LJ.** 2008. DNA repair is crucial for maintaining hematopoietic stem cell function. *DNA Repair* **7**, 523–529.

- Nowosielska A.** 2007. Bacterial DNA repair genes and their eukaryotic homologues: 5. The role of recombination in DNA repair and genome stability. *Acta Biochimica Polonica* **54**, 483–494.
- Odahara M, Inouye T, Fujita T, Hasebe M, Sekine Y.** 2007. Involvement of mitochondrial-targeted RecA in the repair of mitochondrial DNA in the moss, *Physcomitrella patens*. *Genes and Genetic Systems* **82**, 43–51.
- Oldenburg DJ, Bendich AJ.** 1996. Size and structure of replicating mitochondrial DNA in cultured tobacco cells. *The Plant Cell* **8**, 447–461.
- Oldenburg DJ, Bendich AJ.** 1998. The structure of mitochondrial DNA from the liverwort, *Marchantia polymorpha*. *Journal of Molecular Biology* **276**, 745–758.
- Oldenburg DJ, Bendich AJ.** 2004a. Changes in the structure of DNA molecules and the amount of DNA per plastid during chloroplast development in maize. *Journal of Molecular Biology* **344**, 1311–1330.
- Oldenburg DJ, Bendich AJ.** 2004b. Most chloroplast DNA of maize seedlings in linear molecules with defined ends and branched forms. *Journal of Molecular Biology* **335**, 953–970.
- Oldenburg DJ, Rowan BA, Zhao L, Walcher CL, Schleh M, Bendich AJ.** 2006. Loss or retention of chloroplast DNA in maize seedlings is affected by both light and genotype. *Planta* **225**, 41–55.
- Pang Q, Hays JB, Rajagopal I.** 1992. A plant cDNA that partially complements *Escherichia coli* recA mutations predicts a polypeptide not strongly homologous to RecA proteins. *Proceedings of the National Academy of Sciences, USA* **89**, 8073–8077.
- Pang Q, Hays JB, Rajagopal I, Schaefer TS.** 1993. Selection of Arabidopsis cDNAs that partially correct phenotypes of *Escherichia coli* DNA-damage-sensitive mutants and analysis of two plant cDNAs that appear to express UV-specific dark repair activities. *Plant Molecular Biology* **22**, 411–426.
- Pitcher RS, Brissett NC, Doherty AJ.** 2007. Nonhomologous end-joining in bacteria: a microbial perspective. *Annual Review of Microbiology* **61**, 259–282.
- Prina A.** 1992. A mutator nuclear gene inducing a wide spectrum of cytoplasmically inherited chlorophyll deficiencies in barley. *Theoretical and Applied Genetics* **85**, 245–251.
- Raji H, Hartsuiker E.** 2006. Double-strand break repair and homologous recombination in *Schizosaccharomyces pombe*. *Yeast* **23**, 963–976.
- Redei GP, Plurad SB.** 1973. Hereditary structural alterations of plastids induced by a nuclear mutator gene in Arabidopsis. *Protoplasma* **77**, 361–380.
- Riha K, McKnight TD, Griffing LR, Shippen DE.** 2001. Living with genome instability: plant responses to telomere dysfunction. *Science* **291**, 1797–1800.
- Rocha EP, Cornet E, Michel B.** 2005. Comparative and evolutionary analysis of the bacterial homologous recombination systems. *PLoS Genetics* **1**, e15.
- Roldan-Arjona T, Ariza RR.** 2009. Repair and tolerance of oxidative DNA damage in plants. *Mutation Research* **681**, 169–179.
- Rowan BA, Oldenburg DJ, Bendich AJ.** 2004. The demise of chloroplast DNA in Arabidopsis. *Current Genetics* **46**, 176–181.
- Rowan BA, Oldenburg DJ, Bendich AJ.** 2007. A high-throughput method for detection of DNA in chloroplasts using flow cytometry. *Plant Methods* **3**, 5.
- Rowan BA, Oldenburg DJ, Bendich AJ.** 2009. A multiple-method approach reveals a declining amount of chloroplast DNA during development in Arabidopsis. *BMC Plant Biology* **9**, 3.
- Sakamoto W, Kondo H, Murata M, Motoyoshi F.** 1996. Altered mitochondrial gene expression in a maternal distorted leaf mutant of Arabidopsis induced by chloroplast mutator. *The Plant Cell* **8**, 1377–1390.
- Sancar A, Sancar GB.** 1988. DNA repair enzymes. *Annual Review of Biochemistry* **57**, 29–67.
- Scharff LB, Koop HU.** 2006. Linear molecules of tobacco ptDNA end at known replication origins and additional loci. *Plant Molecular Biology* **62**, 611–621.
- Shaver JM, Oldenburg DJ, Bendich AJ.** 2006. Changes in chloroplast DNA during development in tobacco, *Medicago truncatula*, pea, and maize. *Planta* **224**, 72–82.
- Shaver JM, Oldenburg DJ, Bendich AJ.** 2008. The structure of chloroplast DNA molecules and the effects of light on the amount of chloroplast DNA during development in *Medicago truncatula*. *Plant Physiology* **146**, 1064–1074.
- Shedge V, Arrieta-Montiel M, Christensen AC, Mackenzie SA.** 2007. Plant mitochondrial recombination surveillance requires unusual RecA and MutS homologs. *The Plant Cell* **19**, 1251–1264.
- Skarstad K, Boye E.** 1993. Degradation of individual chromosomes in recA mutants of *Escherichia coli*. *Journal of Bacteriology* **175**, 5505–5509.
- Tarsounas M, West SC.** 2005. Recombination at mammalian telomeres: an alternative mechanism for telomere protection and elongation. *Cell Cycle* **4**, 672–674.
- Thompson LH, Schild D.** 2001. Homologous recombinational repair of DNA ensures mammalian chromosome stability. *Mutation Research* **477**, 131–153.
- Trifunovic A, Larsson NG.** 2008. Mitochondrial dysfunction as a cause of ageing. *Journal of Internal Medicine* **263**, 167–178.
- Tuteja N, Ahmad P, Panda BB, Tuteja R.** 2009. Genotoxic stress in plants: shedding light on DNA damage, repair and DNA repair helicases. *Mutation Research* **681**, 134–149.
- Vlcek D, Sevcovicova A, Sviezena B, Galova E, Miadokova E.** 2008. *Chlamydomonas reinhardtii*: a convenient model system for the study of DNA repair in photoautotrophic eukaryotes. *Current Genetics* **53**, 1–22.
- Wall MK, Mitchenall LA, Maxwell A.** 2004. Arabidopsis thaliana DNA gyrase is targeted to chloroplasts and mitochondria. *Proceedings of the National Academy of Sciences, USA* **101**, 7821–7826.
- Yu F, Fu A, Aluru M, Park S, Xu Y, Liu H, Liu X, Foudree A, Nambogga M, Rodermeil S.** 2007. Variegation mutants and mechanisms of chloroplast biogenesis. *Plant, Cell and Environment* **30**, 350–365.